Excitation energies of pi-conjugated oligomers within time-dependent current-density-functional theory

van Faassen, M.; de Boeij, P. L.

Excitation energies of π-conjugated oligomers within time-dependent current-density-functional theory

M. van Faassen and P. L. de Boeij
Theoretical Chemistry, Materials Science Centre, Rijksuniversiteit Groningen, Nijenborgh 4,
9747 AG Groningen, The Netherlands

We study the $\pi^* \leftarrow \pi$ singlet excitations of the π-conjugated oligomers of polyacetylene, polydiacetylene, polybutatriene, polythiophene, poly(*para*-phenylene vinylene), and the lowest singlet excitations of the hydrogen chain. For this we used time-dependent current-density-functional theory within the Vignale–Kohn and adiabatic local density approximations. By studying the dependence of the excitation spectrum on the chain length we conclude that the reduction of the static polarizability when using the Vignale–Kohn functional has two origins. First, the excitation energies of transitions with a large transition dipole are shifted upward. Second, the character of the transition between the lowest occupied and highest unoccupied molecular orbitals and the oscillator strength of the lowest transition within the adiabatic local density approximation is transferred to higher transitions. The lowest transitions that have a considerable oscillator strength obtained with the Vignale–Kohn functional have excitation energies that are in most cases in better agreement with available reference data than the adiabatic local density approximation. © *2004 American Institute of Physics.* [DOI: 10.1063/1.1810137]

I. INTRODUCTION

Time-dependent density-functional theory[1–3] is an exact theory to describe the dynamical response of many-particle systems to external perturbations. In this effective one-particle scheme many-particle effects enter via a so-called exchange-correlation potential. The standard adiabatic local density approximation (ALDA) for this exchange-correlation potential often gives accurate results for polarizabilities and excitation energies (many references are given in Ref. 4). However, in some cases this simple approximation does not suffice. Important examples are the static axial polarizability and hyperpolarizability of conjugated oligomers, which are greatly overestimated within the ALDA. This local approximation and also more advanced generalized gradient approximations are unable to describe the highly nonlocal exchange and correlation effects found in these quasi-one-dimensional systems.[5,6] Several methods are available to overcome this problem.[7–10] In our previous works, Refs. 11 and 12, we have found a successful alternative approach towards the solution of this longstanding problem. We use time-dependent current-density-functional theory (TD-CDFT), in which we describe ultranonlocal exchange-correlation effects using a functional that is dependent on the current density. Vignale and Kohn (VK) proposed such a functional[13,14] in which the current density is used as a local indicator of global changes. From a careful analysis of the weakly inhomogeneous perturbed electron gas they arrived at an expression[13–16] for the first-order induced exchange-correlation contributions in the form of a viscoelastic stress field. Within the VK functional we use a parametrization of the viscoelastic coefficient based on results of Conti, Nifosì, and Tosi[17] for the transverse response of the homogeneous electron gas.[11] For the prototype polyacetylene and many

other linear conjugated oligomers the results obtained using this VK functional significantly improved upon the ALDA results, and were in excellent agreement with high level *ab initio* quantum chemical methods. However, we also observed that a similar large correction was not obtained for a hydrogen chain with alternating bond lengths, which is seen as a theoretical model for conjugated systems (see Ref. 18 and references therein). This indicates that the VK functional in the parameterization we use is not able to describe all features necessary for a correct description of the axial polarizability.

In Refs. 19 and 20 we calculated the excitation energies of a benchmark set of molecules. We studied several types of transitions. In most cases, the excitation energies of the $\pi^* \leftarrow \pi$ transitions obtained with the VK functional were found to improve much upon the ALDA values, giving results close to other values available from literature. We also found that the $\pi^* \leftarrow n$ transitions were strongly overestimated with VK and that for some other types of excitations the picture that emerges was less clear. In the π-conjugated systems studied here the low-lying $\pi^* \leftarrow \pi$ transitions determine for a large part the axial polarizability. We therefore expect that the reduction in the polarizability for these systems is linked to a modification of the $\pi^* \leftarrow \pi$ excitations.

In this paper we study the lowest dipole-allowed singlet excitations of the oligomers of polyacetylene, polydiacetylene, polybutatriene, polythiophene, poly(*para*-phenylene vinylene), and the hydrogen chain. The singlet excitations considered here are all of the $\pi^* \leftarrow \pi$ type except for the hydrogen chain. We will compare our results with available experimental and *ab initio* data. From the results for the $\pi^* \leftarrow \pi$ excitations of the small molecules and the excellent VK results for the polarizabilities of π-conjugated oligo-

mers, we may expect a large improvement with VK upon the calculated ALDA excitation spectra.

II. THEORY

A detailed description of how to calculate excitation energies within time-dependent current-density-functional theory are given in Refs. 19 and 20. There one can also find how to include the VK functional. Here we will only give a brief outline.

We consider the response of a system with a ground state that is described within a spin-restricted formulation. However, we treat the response for each spin component separately. The time-dependent Kohn–Sham equations of TD-CDFT are

$$\{\tfrac{1}{2}[-i\boldsymbol{\nabla}+\mathbf{A}_{\text{eff},\sigma}(\mathbf{r},t)]^2+v_{\text{eff},\sigma}(\mathbf{r},t)\}\phi_{n\sigma}(\mathbf{r},t)$$

$$=i\frac{\partial}{\partial t}\phi_{n\sigma}(\mathbf{r},t), \tag{1}$$

where σ indicates the spin component. The time-dependent effective potentials $v_{\text{eff},\sigma}(\mathbf{r},t)$ and $\mathbf{A}_{\text{eff},\sigma}(\mathbf{r},t)$ are uniquely determined up to an arbitrary gauge transformation by the exact time-dependent density and current density.[21,22] These densities can be obtained from the orbitals $\phi_{n\sigma}(\mathbf{r},t)$ by

$$\rho_\sigma(\mathbf{r},t)=\sum_n n_{n\sigma}\phi^*_{n\sigma}(\mathbf{r},t)\phi_{n\sigma}(\mathbf{r},t) \tag{2}$$

and

$$\mathbf{j}_\sigma(\mathbf{r},t)=\sum_n n_{n\sigma}\frac{-i}{2}[\phi^*_{n\sigma}(\mathbf{r},t)\boldsymbol{\nabla}\phi_{n\sigma}(\mathbf{r},t)$$

$$-\phi_{n\sigma}(\mathbf{r},t)\boldsymbol{\nabla}\phi^*_{n\sigma}(\mathbf{r},t)]+\rho_\sigma(\mathbf{r},t)\mathbf{A}_{\text{eff},\sigma}(\mathbf{r},t). \tag{3}$$

Here $n_{n\sigma}$ are the occupation numbers, where for the spin-restricted case, $n_{n\uparrow}=n_{n\downarrow}=1$ for the occupied states and $n_{n\uparrow}=n_{n\downarrow}=0$ for the unoccupied states. To obtain the excitation energies we use linear response theory.[2,19,20,23,24] The first-order changes in the scalar and vector potentials are then given by

$$\delta v_{\text{eff},\sigma}(\mathbf{r},\omega)=\delta v_H(\mathbf{r},\omega)+\delta v_{\text{xc},\sigma}(\mathbf{r},\omega) \tag{4}$$

and

$$\delta \mathbf{A}_{\text{eff},\sigma}(\mathbf{r},\omega)=\delta \mathbf{A}_{\text{ext}}(\mathbf{r},\omega)+\delta \mathbf{A}_{\text{xc},\sigma}(\mathbf{r},\omega), \tag{5}$$

where $\delta v_H(\mathbf{r},\omega)$ represents the first order change in the Hartree potential, $\delta \mathbf{A}_{\text{ext}}(\mathbf{r},\omega)$ is the perturbing external field, and $\delta v_{\text{xc},\sigma}(\mathbf{r},\omega)$ and $\delta \mathbf{A}_{\text{xc},\sigma}(\mathbf{r},\omega)$ are the first order changes in the spin-dependent scalar and vector xc potentials. We use the Coulomb gauge for the induced Hartree potential. The first-order changes in the xc contribution can be given in the form

$$\delta v_{\text{xc},\sigma}(\mathbf{r},\omega)=\sum_{\sigma'}\int f^{\sigma\sigma'}_{\text{xc}}(\mathbf{r},\mathbf{r}',\omega)\delta\rho_{\sigma'}(\mathbf{r}',\omega)d\mathbf{r}' \tag{6}$$

and

$$\delta \mathbf{A}_{\text{xc},\sigma}(\mathbf{r},\omega)=\sum_{\sigma'}\int \mathbf{f}^{\sigma\sigma'}_{\text{xc}}(\mathbf{r},\mathbf{r}',\omega)\delta\mathbf{j}_{\sigma'}(\mathbf{r}',\omega)d\mathbf{r}', \tag{7}$$

where $f^{\sigma\sigma'}_{\text{xc}}$ and $\mathbf{f}^{\sigma\sigma'}_{\text{xc}}$ are the spin-dependent scalar and tensor xc kernels. For the spin restricted ground state, $f^{\uparrow\uparrow}_{\text{xc}}=f^{\downarrow\downarrow}_{\text{xc}}$, $f^{\uparrow\downarrow}_{\text{xc}}=f^{\downarrow\uparrow}_{\text{xc}}$, $\mathbf{f}^{\uparrow\uparrow}_{\text{xc}}=\mathbf{f}^{\downarrow\downarrow}_{\text{xc}}$, and $\mathbf{f}^{\uparrow\downarrow}_{\text{xc}}=\mathbf{f}^{\downarrow\uparrow}_{\text{xc}}$. For the spin-restricted case we can choose the orbitals to be real, which we will use in the following. We can express the total spin-integrated induced density and induced current density as follows:

$$\delta\rho(\mathbf{r},\omega)=\sum_\sigma\sum_{i,a}\phi_{a\sigma}(\mathbf{r})\phi_{i\sigma}(\mathbf{r})2\,\delta P_{ia\sigma}(\omega), \tag{8}$$

$$\delta\mathbf{j}(\mathbf{r},\omega)=\sum_\sigma\sum_{i,a}\frac{\omega}{(\varepsilon_{i\sigma}-\varepsilon_{a\sigma})}\phi_{a\sigma}(\mathbf{r})\hat{\mathbf{j}}\phi_{i\sigma}(\mathbf{r})2\,\delta P_{ia\sigma}(\omega), \tag{9}$$

where the $\delta P_{ia\sigma}(\omega)$ are the solutions of the following equations:

$$\sum_{jb\tau}\left[\delta_{\sigma\tau}\delta_{ab}\delta_{ij}(\varepsilon_{i\sigma}-\varepsilon_{a\sigma})-2K^{\sigma\tau}_{ia,jb}(\omega)\right.$$

$$\left.-\omega^2\frac{\delta_{\sigma\tau}\delta_{ab}\delta_{ij}}{(\varepsilon_{i\sigma}-\varepsilon_{a\sigma})}\right]\delta P_{jb\tau}(\omega)$$

$$=\frac{\omega}{(\varepsilon_{i\sigma}-\varepsilon_{a\sigma})}\int\phi_{i\sigma}(\mathbf{r})\hat{\mathbf{j}}\phi_{a\sigma}(\mathbf{r})\delta\mathbf{A}_{\text{ext},\sigma}(\mathbf{r},\omega)d\mathbf{r}, \tag{10}$$

with an in general frequency dependent coupling matrix,

$$K^{\sigma\tau}_{ia,jb}(\omega)=\int\int\phi_{i\sigma}(\mathbf{r})\phi_{a\sigma}(\mathbf{r})\left[\frac{1}{|\mathbf{r}-\mathbf{r}'|}+f^{\sigma\tau}_{\text{xc}}(\mathbf{r},\mathbf{r}',\omega)\right]$$

$$\times\phi_{j\tau}(\mathbf{r}')\phi_{b\tau}(\mathbf{r}')d\mathbf{r}d\mathbf{r}'$$

$$+\frac{-\omega^2}{(\varepsilon_{i\sigma}-\varepsilon_{a\sigma})(\varepsilon_{j\sigma}-\varepsilon_{b\sigma})}\int\int\phi_{i\sigma}(\mathbf{r})\hat{\mathbf{j}}\phi_{a\sigma}(\mathbf{r})$$

$$\times\mathbf{f}^{\sigma\tau}_{\text{xc}}(\mathbf{r},\mathbf{r}',\omega)\phi_{j\tau}(\mathbf{r}')\hat{\mathbf{j}}\phi_{b\tau}(\mathbf{r}')d\mathbf{r}d\mathbf{r}'. \tag{11}$$

In the above equations i runs over the occupied states and a over the unoccupied states and σ and τ are the corresponding spin variables. If the ALDA is used for the scalar xc-kernel $f^{\sigma\tau}_{\text{xc}}$ and if for the tensor xc-kernel $\mathbf{f}^{\sigma\tau}_{\text{xc}}$ one approximates $\mathbf{f}_{\text{xc}}(\mathbf{r},\mathbf{r}',\omega)=c(\mathbf{r},\mathbf{r}')/\omega^2$, where $c(\mathbf{r},\mathbf{r}')=\lim_{\omega\to 0}\omega^2\mathbf{f}_{\text{xc}}(\mathbf{r},\mathbf{r}',\omega)$ the coupling matrix becomes frequency independent. This is the approximation we use. In general, however, the tensor xc-kernel will have a more complicated frequency dependence. In order to preserve the causal structure of the response equations the Kramers–Kronig relation requires that the kernel will have both real and imaginary components. In our approximation we assume that the imaginary component is small and can be neglected for the calculation of excitation energies. This approximation is in keeping with a weak frequency dependence of the real part of $\omega^2\mathbf{f}_{\text{xc}}(\mathbf{r},\mathbf{r}',\omega)$.

In Refs. 19 and 20 we arrive at the following eigenvalue equation from which the excitation energies and oscillator strengths can be obtained,

$$\Omega\mathbf{F}_n=\omega^2_n\mathbf{F}_n, \tag{12}$$

J. Chem. Phys., Vol. 121, No. 21, 1 December 2004

Excitation energies of π-conjugated oligomers   10709

where the ω_n are the excitation energies. The elements of $\mathbf{F}$ are given by

$$F_{ia\sigma} = \frac{1}{\sqrt{\varepsilon_{a\sigma} - \varepsilon_{i\sigma}}} 2\,\delta P_{ia\sigma}(\omega). \tag{13}$$

For a spin-restricted calculation the Ω matrix can be split into a singlet and triplet part by a unitary transformation giving for the components of the four-index matrices Ω^S and Ω^T,

$$\Omega^S_{ia,jb} = \delta_{ij}\delta_{ab}(\varepsilon_a - \varepsilon_i)^2 + 2\sqrt{\varepsilon_a - \varepsilon_i}(K^{\uparrow\uparrow}_{ia,jb} + K^{\uparrow\downarrow}_{ia,jb})$$
$$\times \sqrt{\varepsilon_b - \varepsilon_j}, \tag{14}$$

$$\Omega^T_{ia,jb} = \delta_{ij}\delta_{ab}(\varepsilon_a - \varepsilon_i)^2 + 2\sqrt{\varepsilon_a - \varepsilon_i}(K^{\uparrow\uparrow}_{ia,jb} - K^{\uparrow\downarrow}_{ia,jb})$$
$$\times \sqrt{\varepsilon_b - \varepsilon_j}. \tag{15}$$

We can relate the right-hand side of Eq. (10) to the dipole matrix elements,

$$\int \phi_{i\sigma}(\mathbf{r})\hat{\mathbf{r}}\phi_{a\sigma}(\mathbf{r})d\mathbf{r} = \frac{i}{(\varepsilon_{a\sigma} - \varepsilon_{i\sigma})}\int \phi_{i\sigma}(\mathbf{r})\hat{\mathbf{j}}\phi_{a\sigma}(\mathbf{r})d\mathbf{r}. \tag{16}$$

It then becomes clear that our equations are very similar to those derived by Casida;[25] we only need to use a different coupling matrix to include the current functional. We compare the expression for the polarizability from TDCDFT with the sum-over-states (SOS) expression,

$$\bar{\alpha}(\omega) = \sum_n \frac{f_n}{\omega_n^2 - \omega^2}. \tag{17}$$

For the oscillator strengths we can use Casida's result,

$$f_n = \frac{2}{3}(|\mathbf{x}^\dagger\mathbf{S}^{-1/2}\mathbf{F}_n|^2 + |\mathbf{y}^\dagger\mathbf{S}^{-1/2}\mathbf{F}_n|^2 + |\mathbf{z}^\dagger\mathbf{S}^{-1/2}\mathbf{F}_n|^2), \tag{18}$$

where the elements of $\mathbf{x}$, $\mathbf{y}$, and $\mathbf{z}$ are the three Cartesian components of the dipole matrix elements of Eq. (16), and

$$S^{-1/2}_{ia\sigma,jb\tau} = \delta_{\sigma\tau}\delta_{ab}\delta_{ij}\sqrt{\varepsilon_{a\sigma} - \varepsilon_{i\sigma}} \tag{19}$$

is a diagonal matrix. We made use of the fact that our Ω matrix is frequency independent, and we chose the $\mathbf{F}$s to be normalized. From this result one can see that we can obtain the transition dipole moment in the x direction from,

$$\langle \Psi_0|\hat{x}|\Psi_n\rangle = \mathbf{x}^\dagger\mathbf{S}^{-1/2}\mathbf{F}_n\omega_n^{-1/2} \tag{20}$$

and similar for the y and z directions. Until now we made no reference to any wave function. In order to assign the states Ψ_n some assumptions do need to be made on the ground-state wave function. Casida[25] proposes to assume that Ψ_0 is a single determinant Φ of Kohn–Sham orbitals and that the matrix elements of the dipole operator are linearly independent. Equation (20) then becomes (in the notation of second quantization),

$$(\mathbf{S}^{-1/2}\mathbf{F}_n)_{ia\sigma} = \sqrt{\varepsilon_{a\sigma} - \varepsilon_{i\sigma}}\mathbf{F}_n$$
$$= \omega_n^{1/2}\langle \Phi|\hat{a}^\dagger_{i\sigma}\hat{a}_{a\sigma}|\Psi_n\rangle. \tag{21}$$

This determines the coefficients of the singly excited configurations in the following expansion of the excited state:

$$\Psi_n = \sum_{ia\sigma}^{f_{i\sigma} - f_{a\sigma} > 0} \sqrt{\frac{\varepsilon_{a\sigma} - \varepsilon_{i\sigma}}{\omega_n}} F^n_{ia\sigma}\hat{a}^\dagger_{a\sigma}\hat{a}_{i\sigma}\Phi + \cdots. \tag{22}$$

Within the RESPONSE code of the Amsterdam density-functional program package ADF,[26–31] which we will use for our calculations, a further assumption is made. Namely that the excitation energies are close to the Kohn–Sham orbital energy differences, thus that the $F^n_{ia\sigma}$ can be interpreted as the expansion coefficients in Eq. (22). This assumption is not expected to have a large effect on the qualitative trends of the assignments.

As mentioned above we will use the ALDA for the scalar xc-kernel $f^{\sigma\tau}_{xc}$. For the tensor xc-kernel $\mathbf{f}^{\sigma\tau}_{xc}$ we will choose the VK functional.[13,14] It has been shown by Vignale, Ullrich, and Conti[15,32] that for the spin-independent case the VK expression for the total xc contribution can be written in the form of a viscoelastic field. The spin-dependent description of the VK functional is given by[33,34]

$$\delta\mathbf{E}_{xc,\sigma}(\mathbf{r},\omega) = \nabla\,\delta v^{ALDA}_{xc,\sigma}(\mathbf{r},\omega) + i\omega\,\delta\mathbf{A}^{viscoel.}_{xc,\sigma}(\mathbf{r},\omega)$$
$$- \frac{i\rho_0(\mathbf{r})^2 A(\omega)}{4\omega}\sum_{\sigma'} \frac{\sigma\sigma'}{\rho_{0,\sigma}(\mathbf{r})\rho_{0,\sigma'}(\mathbf{r})}\delta\mathbf{j}_{\sigma'}(\mathbf{r},\omega), \tag{23}$$

where $\sigma = +1$ for spin up and $\sigma = -1$ for spin down. The third term of Eq. (23) vanishes in the spin-restricted singlet case. The first two terms in this expression are the ALDA contribution and the viscoelastic force term. The former is obtained using the ALDA expression for the scalar xc-kernel,

$$f^{\sigma\tau}_{xc,ALDA}(\mathbf{r},\mathbf{r}',\omega) = \delta(\mathbf{r} - \mathbf{r}')\left.\frac{\partial v^\sigma_{xc,LDA}}{\partial\rho_\tau}\right|_{\rho_\tau = \rho_{0,\tau}}, \tag{24}$$

while the latter is related to the viscoelastic stress tensor $\sigma_{xc,\sigma}(\mathbf{r},\omega)$ by

$$\delta A^{viscoel.}_{xc,\sigma,i}(\mathbf{r},\omega) = \frac{i}{\omega\rho_0(\mathbf{r})}\sum_j \partial_j\sigma_{xc,\sigma,ij}(\mathbf{r},\omega), \tag{25}$$

$$\sigma_{xc,\sigma,ij}(\mathbf{r},\omega) = \sum_{\sigma'}\left\{\tilde{\eta}^{\sigma\sigma'}_{xc}(\mathbf{r},\omega)\left[\partial_j u_{\sigma',i}(\mathbf{r},\omega)\right.\right.$$
$$\left. + \partial_i u_{\sigma',j}(\mathbf{r},\omega) - \frac{2}{3}\delta_{ij}\nabla\cdot\mathbf{u}_{\sigma'}(\mathbf{r},\omega)\right]$$
$$\left. + \tilde{\zeta}^{\sigma\sigma'}_{xc}(\mathbf{r},\omega)\delta_{ij}\nabla\cdot\mathbf{u}_{\sigma'}(\mathbf{r},\omega)\right\}. \tag{26}$$

In this expression $\mathbf{u}_\sigma(\mathbf{r},\omega) = \delta\mathbf{j}_\sigma(\mathbf{r},\omega)/\rho_{0,\sigma}(\mathbf{r})$ is the velocity field, in which $\delta\mathbf{j}_\sigma(\mathbf{r},\omega)$ is the induced current density. We will use the VK functional in the static limit ($\omega \to 0$). As we explained in Refs. 19 and 20 the coefficient $\omega\tilde{\zeta}^{\sigma\sigma'}_{xc}(\omega)$ vanishes in this limit. In this paper we will only consider singlet excitations. The coefficient $\tilde{\eta}^S_{xc}(\omega)$ for the singlet excitation is identical to the $\tilde{\eta}_{xc}(\omega)$ of the spin-independent case which we used before in our response calculations[11,12] and is in the static limit only dependent on the transverse xc-kernel $f^{\sigma\sigma'}_{xcT}(k,\omega = 0)$ for which we will use the parametrization of Nifosí, Conti, and Tosi.[35] The static limit can only be used if indeed the frequency dependence of the longitudinal and

transverse xc kernels of the electron gas is weak. For frequencies much smaller than the local plasma frequency ω_p of the relevant density region, this approximation is reasonable.[17,36] In case of the $\pi^* \leftarrow \pi$ transitions in the oligomers that we study here this relevant region is the valence region with $r_s \approx 1$ and hence $\omega_p \approx 47$ eV, which is much larger than the typical excitation energies we find. Nevertheless, it will be worthwhile to investigate the influence of the frequency dependence of the viscoelastic coefficients on the excitation energies as new terms appear in the functional. For technical reasons we can presently only include real valued xc kernels. We will use the static limit since including the frequency dependence of the real part of the electron-gas kernel will destroy the causal structure of the response equations.

III. COMPUTATIONAL DETAILS

All calculations were performed with our modified version of ADF.[26–31]

For the oligomers of polyacetylene (PA), polydiacetylene (PDA), polythiophene (PT), and the hydrogen chain we use the same geometry as we used in Ref. 11. For the polybutatriene oligomers we use the same geometry as we used in Ref. 12. This is the first time we study the poly(*para*-phenylene vinylene) (PPV) oligomers. We did a geometry optimization for these oligomers with a generalized gradient approximated potential by Becke[37] for exchange and Perdew[38] for correlation (BP functional). We forced the oligomer geometries to be planar (C_s symmetry).

All calculations were done within the standard ADF TZ2P basis set, which is a triple ζ Slater type basis set augmented with two polarization functions. Cores were kept frozen for carbon up to $1s$ and for sulfur up to $2p$.

In all excitation energy calculations the ground state has been calculated with the local-density approximation (LDA) functional in the VWN parametrization.[39] The response calculations themselves were done with the ALDA derived from the ground-state LDA expression and the VK functional. For the latter we use a parametrization of the viscoelastic coefficient based on results of Conti *et al.*[17] for the transverse response of the homogeneous electron gas.[11] From now on we denote these calculations simply as ALDA and VK instead of LDA/ALDA and LDA/VK.

IV. RESULTS

We will first discuss the prototype PA chain. In Ref. 11 we obtained axial polarizabilities for the PA oligomers that were very close to the available MP2 results if we use the VK functional, but that were considerably overestimated when using the ALDA functional. In Fig. 1 we plot the ALDA and VK results for the (dipole allowed) ^1B_u excitation energies and corresponding oscillator strengths against the number of oligomer (C_2H_2) units. We compare our data with experimental results[40] and CCSD-EOM results.[41] The $1\,^1B_u$ excitation energies obtained within the ALDA are close to the CCSD results for the small chain lengths (3–4 U), but for the longer chains the excitation energies are underestimated. The underestimation for the longest chain of
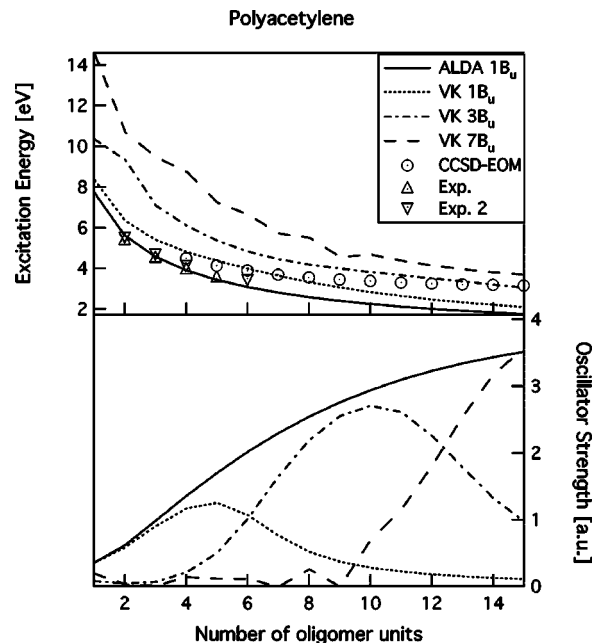

FIG. 1. ALDA and VK excitation energies and oscillator strengths of polyacetylene oligomers compared with CCSD-EOM (Ref. 41) and experimental results. Experiments 1 and 2 are both absorption spectra from Ref. 40.

15 U is 1.39 eV. This result is consistent with the fact that the ALDA overestimates the polarizability as can be seen from the SOS expression for the polarizability, Eq. (17). The reduction of the static polarizability by using the VK functional has to be a result of a decrease of the oscillator strength of the lowest transitions or an increase of their excitation energies, or both. We therefore expect that the excitation energies calculated with VK will improve upon the ALDA. Indeed the VK results for the $1\,^1B_u$ excitation energy are higher than the ALDA results and lie closer to the CCSD results, but from 10 U onward they also underestimate the CCSD results. If we look at the oscillator strengths we see that the ALDA oscillator strength of the $1\,^1B_u$ transition rises, although less steeply for larger chain lengths. This contributes to the large overestimation of the polarizability in case of the ALDA. The VK oscillator strength for the $1\,^1B_u$ transition also rises in the beginning but drops again after 5 U. The $2\,^1B_u$ transition has almost zero oscillator strength for all chain lengths, and for this excitation the effect of VK on the excitation energies is almost zero with values lying very close to the ALDA values. We have therefore not added this excitation to the graph. The oscillator strength of the $3\,^1B_u$ transition with VK rises at the point where the $1\,^1B_u$ oscillator strength drops. The $3\,^1B_u$ oscillator strength drops from 10 U onward, but then the $7\,^1B_u$ transition takes over. The $4\,^1B_u$, $5\,^1B_u$, and $6\,^1B_u$ transitions have again an oscillator strength close to zero and the VK excitation energies are close to their corresponding ALDA values. In Fig. 2 we show the highest occupied molecular orbital-lowest unoccupied molecular orbital (HOMO-LUMO) character and the transition dipole moment in the axial direction for the ^1B_u transition. The transition dipole moment, which is mainly in the axial direction, follows the same trend as the oscillator strengths. If we look at the HOMO-LUMO character we find
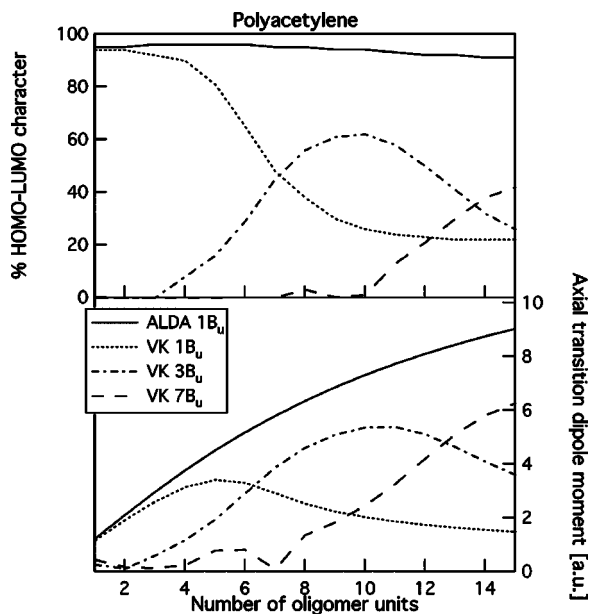
FIG. 2. ALDA and VK HOMO-LUMO character and transition dipole moments for polyacetylene oligomers.
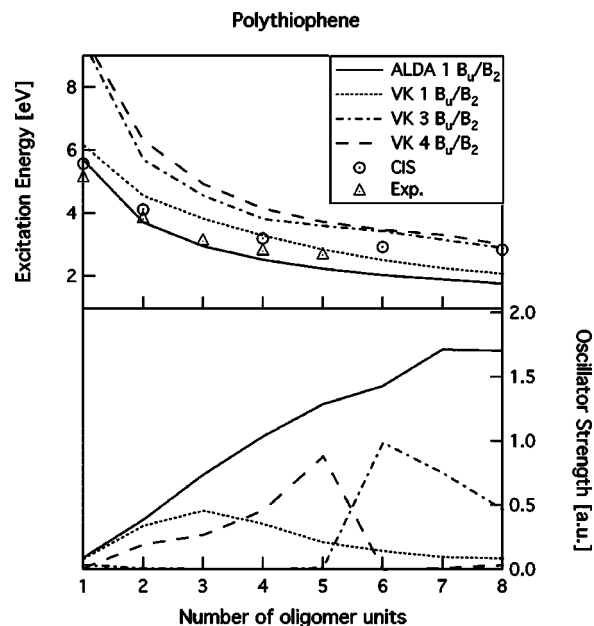

FIG. 3. ALDA and VK excitation energies and oscillator strengths of polythiophene oligomers compared with CIS (Ref. 42) and experimental results (monomer and dimer from Ref. 43, tetramer and seximer from Ref. 44, and octamer from Ref. 45).

that the $1\,^1B_u$ transition has almost 100% HOMO-LUMO within the ALDA. The character of the $1\,^1B_u$ transition with VK is also close to 100% HOMO-LUMO for the small chains, but when the chains become longer more states mix in. Just like in case of the oscillator strength are the $3\,^1B_u$ and later the $7\,^1B_u$ transitions that gain HOMO-LUMO character. We see that the excitations with a large spectral weight are not the lowest transitions with VK and they move to higher energy as the chain becomes longer. These transitions with the largest spectral weight lie close to the CCSD results. This is consistent with the fact that we find much lower polarizabilities for PA with VK.

In Fig. 3 we show the excitation energies and oscillator strengths for the $1\,^1B_u$ (even number of thiophene rings) and $1\,^1B_2$ (odd number of thiophene rings) transitions of PT against the number of SC_4H_2 units. The ALDA and VK results show the same behavior as observed for PA. The oscillator strength of the $1\,^1B_u/^1B_2$ transition of VK drops for longer chain lengths and the spectral weight is transferred to the $3\,^1B_u/^1B_2$ and $4\,^1B_u/^1B_2$ transitions. The $2\,^1B_u/^1B_2$ transition in between again has almost zero oscillator strength and the VK excitation energies lie close to the ALDA values. For the axial transition dipole moment and the HOMO-LUMO character we see the same trends as for polyacetylene, specifically the axial transition dipole moment shows the same trend as the oscillator strength and with VK the HOMO-LUMO character is transferred from the $1\,^1B_u/^1B_2$ to the $3\,^1B_u/^1B_2$ and later to the $4\,^1B_u/^1B_2$ transition. If we compare our results with the available CIS[42] and experimental[43-45] results it is clear that the ALDA underestimates the excitation energies for the long chain lengths. The VK results for the transitions with the largest oscillator strengths lie close to the CIS and experimental results, which is consistent with our earlier observations for the polarizability.[11]

In Ref. 12 we made a comparison for the polarizabilities

of the oligomers of PDA and polybutatriene (PBT). We found that the polarizabilties obtained with VK of these two systems are very similar. The value per oligomer unit, which can be estimated from the experimental values for the polydiacetylenelike PTS ($R=R'=CH_2-O-SO_2-C_6H_4-CH_3$) and polybutatrienelike TDCU ($R=R'=(CH_2)_4-O-CO-NH-C_6H_5$), are also found to be close together.[46] The Hartree–Fock polarizabilities for these systems were very different, the PDA result lying close to our VK values but the PBT value being much larger for the larger chains. Some CASSCF and CASPT2 results for the $1\,^1A'$ excitation energies of PDA and the $1\,^1B_u$ excitation energies of PDA were available from the literature for the shorter chains.[47] The CASPT2 values are considered the most accurate according to Ref. 47. There are also CCSD results available for the monomers.[48] We show these results together with our VK and ALDA results in Figs. 4 and 5. The oligomer unit is for both molecules a C_4H_2 unit. The trends observed for the ALDA and VK excitation energies, oscillator strengths, HOMO-LUMO character, and axial transition dipole moments are again similar to the previous examples. In case of PDA the CASPT2 and CASSCF results for the excitation energies lie close to the VK values with the largest oscillator strength. For PBT the CASSCF results lie close to the VK results with the largest oscillator strength, but here the CASPT2 results lie closer to the ALDA. The literature data for PBT are widely spread for the longer chain lengths, and we cannot make any conclusions on weather the VK results improve upon the ALDA. As can be seen from Fig. 5 the oscillator strength for the $3\,^1B_u$ transition of butatriene (1 U of PBT) with VK is larger than the oscillator strength of the $1\,^1B_u$ transition, but it turns out that the stronger $3\,^1B_u$ excitation does not correspond to a HOMO-LUMO excitation with VK. The major contribution to this transition is from the HOMO$-1\rightarrow$LUMO$+1$. Therefore the $3\,^1B_u$ transition of
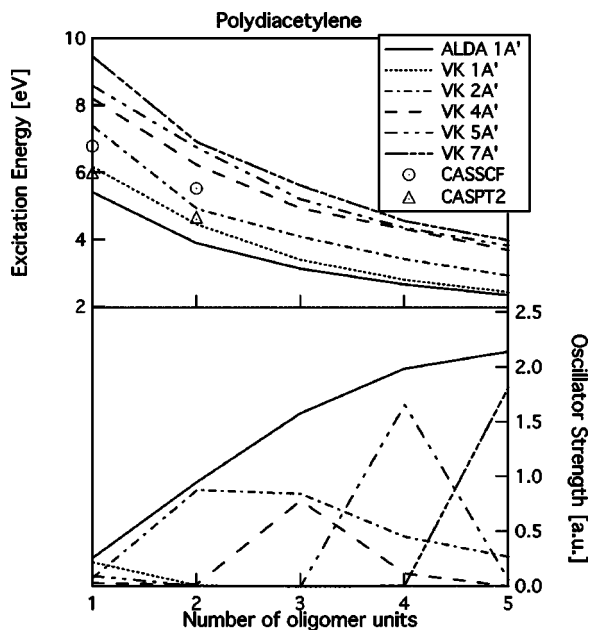
FIG. 4. ALDA and VK excitation energies and oscillator strengths of poly-diacetylene oligomers compared with CASSCF (Ref. 47), CASPT2 (Ref. 47) results.
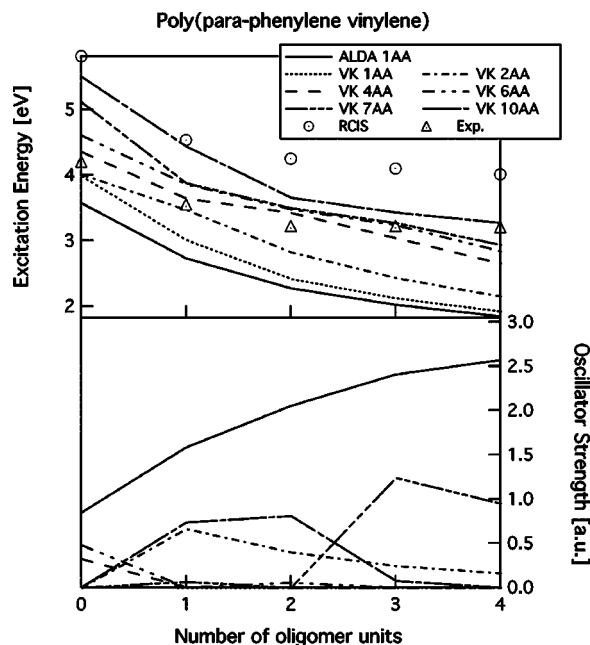

FIG. 6. ALDA and VK excitation energies and oscillator strengths of poly(*para*-phenylene vinylene) oligomers compared with RCIS (Ref. 50) and experimental (Ref. 49) results.

VK should be compared with the $3\,^1B_u$ transition of the ALDA (7.58 eV for the excitation energy and 1.21 a.u. for the oscillator strength).

In Fig. 6 we show the results for poly(*para*-phenylene vinylene) (PPV). We choose the *trans*-stilbene molecule to be zero PPV units, a new unit is obtained by adding a styrene unit between the *trans*-stilbene. It is immediately clear from the figures that with VK many states mix in. We see again the same trends as for the other systems studied. The ALDA values for the excitation energies strongly underestimate the experimental[49] and RCIS[50] results, especially for the longer

chain lengths. The excitation energies with VK for the transitions with the largest oscillator strengths are all in between the experimental and RCIS results, the longer chains being closer to the experimental values.

Finally we studied the hydrogen chain. In Ref. 11 we showed that VK has hardly any effect on the polarizability of the model hydrogen chain. In Figs. 7 and 8 we show our results for the $^1A_{2u}$ transition for ALDA and VK. We see that VK has hardly any effect on the excitation energies of the hydrogen chain. For the really long chains the $3\,^1A_{2u}$ transition takes over from the $1\,^1A_{2u}$ transition for VK but the
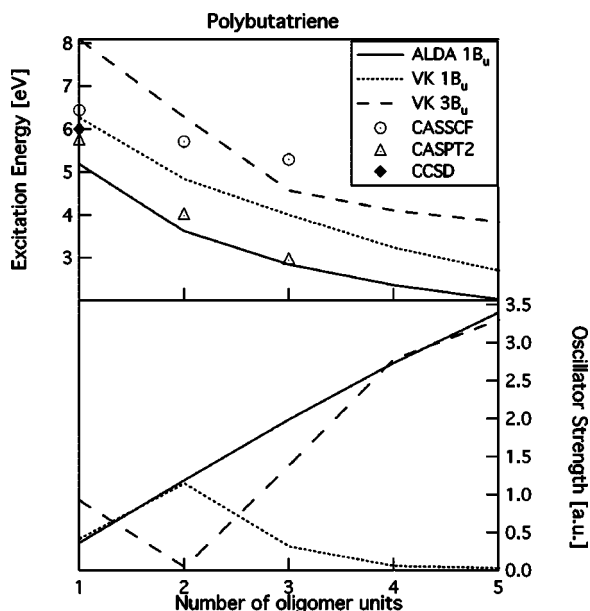

FIG. 5. ALDA and VK excitation energies and oscillator strengths of po-lybutatriene oligomers compared with CASSCF and CASPT2 results (Ref. 47), and STEOM-CCSD (Ref. 48) results.
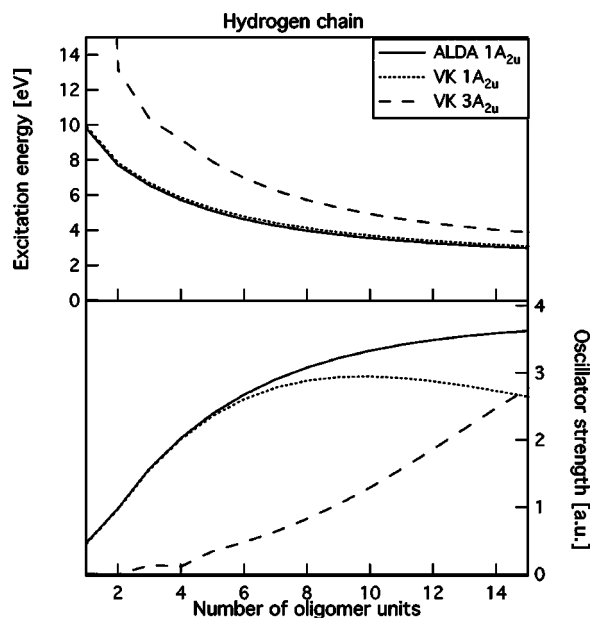

FIG. 7. ALDA and VK excitation energies and oscillator strengths of the hydrogen chain.
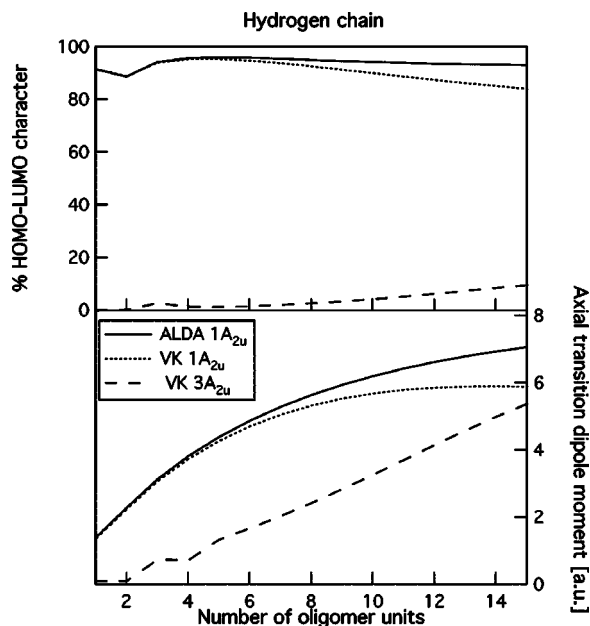
FIG. 8. ALDA and VK HOMO-LUMO character and transition dipole moments for the hydrogen chain.

FIG. 9. ALDA and VK excitation energies and oscillator strengths of polyacetylene.

effect is small. If we look at the HOMO-LUMO character we see that even for the long chains the HOMO-LUMO character is still >90% with VK.

V. DISCUSSION

For all systems studied here we see the same trends. With VK the oscillator strength, axial transition dipole moment and HOMO-LUMO character are transferred to higher states. In all cases the excitation energies obtained with VK lie higher than the ALDA values. Except for the hydrogen chain model and PBT the excitation energies obtained with VK that have the largest spectral weight are closer to the available literature results. This explains why we obtain lower values for the polarizability with VK. However the individual excitation energies and oscillator strengths are not correctly described with VK.

In Fig. 9 we again show the excitation energies and oscillator strengths of PA, but this time we added all transitions up to $4\,^1B_u$ for both ALDA and VK (to keep the graph readable we do not show the higher transitions). The ALDA and VK energies for the $2\,^1B_u$ and $4\,^1B_u$ transitions lie very close together. As mentioned the oscillator strengths for these transitions are very small. The $1\,^1B_u$ transition of VK moves away from the $1\,^1B_u$ transition of the ALDA until it comes close to the $2\,^1B_u$ transition. We see that at this point the $3\,^1B_u$ transition starts to move away from the ALDA, as if the $1\,^1B_u$ transition "pushes through" the $2\,^1B_u$ transition. We observe the same phenomenon when the $3\,^1B_u$ transition pushes through the $4\,^1B_u$, $5\,^1B_u$, and $6\,^1B_u$ transitions and becomes the $7\,^1B_u$ transition. We saw in Refs. 19 and 20 that in case of $\pi^*\leftarrow\pi$ transitions a large oscillator strength (and a large transition dipole moment) means a large VK effect. This is exactly what we observe here. The excitation energies with little oscillator strength do not shift compared to the ALDA and the transitions with a large oscillator strength
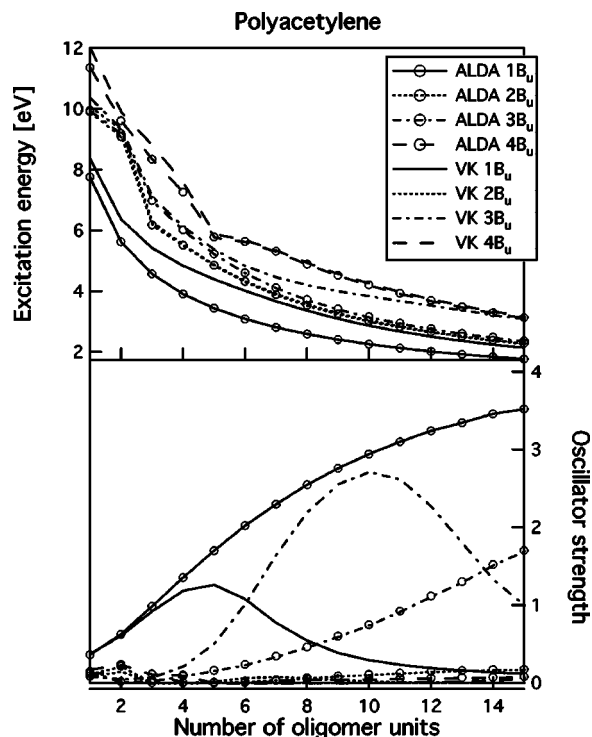
have a large shift compared to the ALDA. We see the same for the other systems studied. We also see in Fig. 9 that the $3\,^1B_u$ transition within the ALDA gains oscillator strength for the long chains. With VK this excitation gets mixed in with several higher states and it is difficult to see which VK state corresponds with the $3\,^1B_u$ transition within the ALDA.

In all systems studied here the excitations with large oscillator strengths also have a large axial transition dipole moment. This means that there is a large global displacement of charge along the long axis of the molecule, which means a large current flow and a large VK effect. The excitations for which the oscillator strengths and transition dipole moments are small have only a small global charge displacement (small current) and therefore the VK effect is small. The problem with VK seems to be that the transitions with small oscillator strengths do not shift upward like the transitions that do have large oscillator strengths. When transitions with large and small oscillator strength become close in energy, they can mix and the oscillator strength becomes distributed over these states. The mean weighed average of the excitation energies is however roughly at the correct position.

VI. CONCLUSION

We calculated the excitation spectra for several π-conjugated oligomers with the VK functional. For these systems we found in our previous studies[11,12] that the axial polarizability obtained with VK lies close to the literature values, while the ALDA strongly overestimates. Previously we also studied the $\pi^*\leftarrow\pi$ transitions of some small π-conjugated systems and found an improvement of the excitation energy when using VK. In this work we find that the

10714   J. Chem. Phys., Vol. 121, No. 21, 1 December 2004

M. van Faassen and P. L. de Boeij

excitation energies, underestimated within the ALDA, are always increased by VK. We also saw that VK transfers the oscillator strength to higher excitations. A remaining problem is that the transitions with small oscillator strengths do not shift upward like the transitions that do have large oscillator strengths. This leads to the fact that individual excitation energies and oscillator strengths are not correctly described with VK. We did observe that the VK transitions that have the largest spectral weight lie close to the available literature results for all systems except PBT and the hydrogen chain.

ACKNOWLEDGMENTS

[1] E. Runge and E. K. Gross, Phys. Rev. Lett. **52**, 997 (1984).
[2] E. K. U. Gross and W. Kohn, Adv. Quantum Chem. **21**, 255 (1990).
[3] R. van Leeuwen, Int. J. Mod. Phys. B **15**, 1969 (2001).
[4] E. K. U. Gross, J. F. Dobson, and M. Petersilka, Top. Curr. Chem. **181**, 81 (1996).
[5] B. Champagne, E. A. Perpète, S. J. A. van Gisbergen, E. J. Baerends, J. G. Snijders, C. Soubra-Ghaoui, K. A. Robins, and B. Kirtman, J. Chem. Phys. **109**, 10489 (1998).
[6] S. J. A. van Gisbergen, P. R. T. Schipper, O. V. Gritsenko, E. J. Baerends, J. G. Snijders, B. Champagne, and B. Kirtman, Phys. Rev. Lett. **83**, 694 (1999).
[7] J. D. Talman and W. G. Shadwick, Phys. Rev. A **14**, 36 (1976).
[8] J. B. Krieger, Y. Li, and G. J. Iafrate, Phys. Rev. A **45**, 101 (1992).
[9] M. Grüning, O. V. Gritsenko, and E. J. Baerends, J. Chem. Phys. **116**, 6435 (2002).
[10] F. Della Sala and A. Görling, J. Chem. Phys. **115**, 5718 (2001).
[11] M. van Faassen, P. L. de Boeij, R. van Leeuwen, J. A. Berger, and J. G. Snijders, Phys. Rev. Lett. **88**, 186401 (2002).
[12] M. van Faassen, P. L. de Boeij, R. van Leeuwen, J. A. Berger, and J. G. Snijders, J. Chem. Phys. **118**, 1044 (2003).
[13] G. Vignale and W. Kohn, Phys. Rev. Lett. **77**, 2037 (1996).
[14] G. Vignale and W. Kohn, in *Electronic Density Functional Theory: Recent Progress and New Directions*, edited by J. F. Dobson, G. Vignale, and M. P. Das (Plenum, New York, 1998).
[15] G. Vignale, C. A. Ullrich, and S. Conti, Phys. Rev. Lett. **79**, 4878 (1997).
[16] G. Vignale, Int. J. Mod. Phys. B **15**, 1714 (2001).
[17] S. Conti, R. Nifosì, and M. P. Tosi, J. Phys.: Condens. Matter **9**, L475 (1997).
[18] B. Champagne, D. H. Mosley, M. Vračko, and J. M. André, Phys. Rev. A **52**, 1039 (1995).
[19] M. van Faassen and P. L. de Boeij, J. Chem. Phys. **120**, 8353 (2004).
[20] M. van Faassen and P. L. de Boeij, J. Chem. Phys. **120**, 11967 (2004).
[21] A. K. Dhara and S. K. Ghosh, Phys. Rev. A **35**, 442 (1987).
[22] S. K. Ghosh and A. K. Dhara, Phys. Rev. A **38**, 1149 (1988).
[23] M. E. Casida, in *Recent Developments and Applications of Modern Density Functional Theory*, edited by J. M. Seminario (Elsevier, Amsterdam, 1996).
[24] S. J. A. van Gisbergen, J. G. Snijders, and E. J. Baerends, Comput. Phys. Commun. **118**, 119 (1999).
[25] M. E. Casida, in *Recent Advances in Density-Funtional Methods*, edited by D. P. Chong (World Scientific, Singapore, 1995), pp. 155.
[26] E. J. Baerends, J. A. Autschbach, A. Bérces *et al.*, ADF2003.01, SCM, Theoretical Chemistry, Vrije Universiteit, Amsterdam, The Netherlands, http://www.scm.com, the version we used in this article was modified by M. van Faassen.
[27] E. J. Baerends, D. E. Ellis, and P. Ros, Chem. Phys. **2**, 41 (1973).
[28] L. Versluis and T. Ziegler, J. Chem. Phys. **88**, 322 (1988).
[29] G. te Velde and E. J. Baerends, J. Comput. Phys. **99**, 84 (1992).
[30] S. J. A. van Gisbergen, J. G. Snijders, and E. J. Baerends, J. Chem. Phys. **103**, 9347 (1995).
[31] C. F. Guerra, J. G. Snijders, G. te Velde, and E. J. Baerends, Theor. Chim. Acta **99**, 391 (1998).
[32] C. A. Ullrich and G. Vignale, Phys. Rev. B **65**, 245102 (2002).
[33] Z. X. Qian and G. Vignale, Phys. Rev. B **68**, 195113 (2003).
[34] Z. Qian, A. Constantinescu, and G. Vignale, Phys. Rev. Lett. **90**, 066402 (2003).
[35] R. Nifosì, S. Conti, and M. P. Tosi, Phys. Rev. B **58**, 12758 (1998).
[36] Z. Qian and G. Vignale, Phys. Rev. B **65**, 235121 (2002).
[37] A. D. Becke, Phys. Rev. A **38**, 3098 (1988).
[38] J. P. Perdew, Phys. Rev. B **33**, 8822 (1986).
[39] S. H. Vosko, L. Wilk, and M. Nusair, Can. J. Phys. **58**, 1200 (1980).
[40] M. F. Granville, B. E. Kohler, and J. Bannon Snow, J. Chem. Phys. **75**, 3765 (1981).
[41] Z. Shuai and J. L. Brédas, Phys. Rev. B **62**, 15452 (2000).
[42] D. Chakraborty and J. B. Lagowski, J. Chem. Phys. **115**, 184 (2001).
[43] J. E. Chadwick and B. E. Kohler, J. Phys. Chem. **98**, 3631 (1994).
[44] R. Colditz, D. Grebner, M. Helbig, and S. Rentsch, Chem. Phys. **201**, 309 (1995).
[45] J. Guay, P. Kasai, A. Diaz, R. Wu, J. M. Tour, and L. H. Dao, Chem. Mater. **4**, 1097 (1992).
[46] E. A. Perpète, B. Champagne, and B. Kirtman, J. Chem. Phys. **107**, 2463 (1997).
[47] M. Turki, T. Barisien, J.-Y. Bigot, and C. Daniel, J. Chem. Phys. **112**, 10526 (2000).
[48] M. Tobita, S. Hirata, and R. J. Bartlett (private communication).
[49] R. A. J. Janssen, in *Primary Photoexcitations in Conjugated Polymers: Molecular Exciton versus Semiconductor Band Model*, edited by N. S. Sariciftci (World Scientific, New York, 1997).
[50] J. B. Lagowski, J. Mol. Struct. **589-590**, 125 (2002).